

Probably Approximately Correct Nonlinear Model Predictive Control (PAC-NMPC)

Adam Polevoy^{1,2}, Marin Kobilarov², Joseph Moore^{1,2}

Abstract—Approaches for stochastic nonlinear model predictive control (SNMPC) typically make restrictive assumptions about the system dynamics and rely on approximations to characterize the evolution of the underlying uncertainty distributions. For this reason, they are often unable to capture more complex distributions (e.g., non-Gaussian or multi-modal) and cannot provide accurate guarantees of performance. In this paper, we present a sampling-based SNMPC approach that leverages recently derived sample complexity bounds to certify the performance of a feedback policy without making assumptions about the system dynamics or underlying uncertainty distributions. By parallelizing our approach, we are able to demonstrate real-time receding-horizon SNMPC with statistical safety guarantees in simulation on a 24-inch wingspan fixed-wing UAV and on hardware using a 1/10th scale rally car.

I. INTRODUCTION

Nonlinear model predictive control (NMPC) has proved to be a powerful approach for controlling high-dimensional, complex robotic systems (e.g., [1], [2], [3], [4]). Nevertheless, although these methods can handle large state spaces, nonlinear dynamics, and system constraints, their performance can be adversely affected by the presence of uncertainty even in the context of real-time replanning [5]. A number of approaches have been proposed to compensate for this marginal robustness, the simplest of which is to generate a feedback policy to track the current receding-horizon plan (e.g., [2]). These approaches, however, do not account for uncertainty or closed-loop performance during the planning process. To address this, approaches such as robust NMPC (RNMPC) and stochastic NMPC (SNMPC) attempt to reason about the response of the policy to disturbances during planning. This is usually accomplished by making simplifying assumptions about the dynamics and disturbances. For instance, in RNMPC, disturbance sets may be approximated by ellipsoids [6], or robustness guarantees may require the existence of a control contraction metric (CCM) [7]; in SNMPC, uncertainty distributions are often approximated via Gaussians [8] or sampling [9].

In this paper, we present a sampling-based SNMPC algorithm capable of controlling stochastic dynamical systems without applying limiting assumptions to the structure of the stochastic dynamics or underlying uncertainty distributions. In addition, our approach leverages recently derived sample complexity bounds [10] to provide a probabilistic guarantee on system performance. More specifically, our algorithm

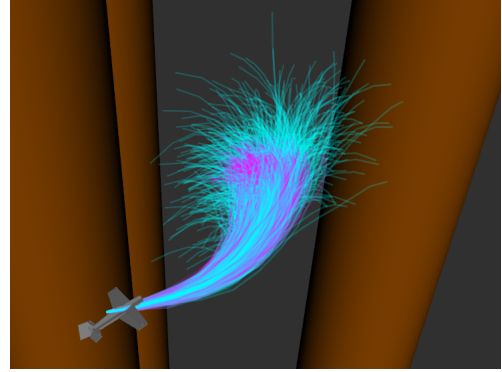


Fig. 1. PAC-NMPC optimizes high confidence bounds on the expected costs/constraint of control trajectory distributions. Samples of trajectories from optimized distributions and stochastic dynamics are shown in cyan. Samples from the means of the optimized distributions and stochastic dynamics are shown in magenta. Obstacles are shown in brown.

builds on Probably Approximately Correct Robust Policy Search (PROPS) [11] to directly optimize an upper confidence bound on the expected cost and the probability of constraint violation for a receding-horizon feedback policy. Not only does this approach encourage robust policy generation, but the minimized bounds themselves provide a statistical guarantee for each planning interval. To achieve real-time performance, we use a graphics processing unit (GPU) to parallelize our algorithm. We then evaluate our approach in simulation on a 24-inch wingspan fixed-wing UAV and in hardware using a 1/10th scale rally car.

Our contributions are:

- A novel algorithm called PAC-NMPC for receding horizon SNMPC with probabilistic performance guarantees.
- A real-time implementation via GPU acceleration.
- Demonstration of our algorithm on complex underactuated systems via simulation and hardware experiments.

II. RELATED WORK

Prior research addresses the impact of uncertainty on NMPC via robust NMPC (RNMPC) or stochastic NMPC (SNMPC). RNMPC represents uncertainty in the system as bounded disturbances. While min-max tube NMPC methods [12], [6], [13] and multi-stage NMPC approaches [14] have been proposed, constraint-tightening based tube NMPC [15] has proved to be the most common and computationally tractable RNMPC approach. Most of these approaches rely on tube size derived from the use of a computed Lipschitz constant [16], [17], CCMs [18], [7], [19], or bounds on incremental stability [20]. These methods for computing invariant sets are often complex, may place significant restrictions on the dynamics, and can lead to overly conservative results.

¹Johns Hopkins University Applied Physics Lab
{Adam.Polevoy, Joseph.Moore}@jhuapl.edu

²Johns Hopkins University
mkobilar1@jhu.edu

Stochastic NMPC represents uncertainty as a probability distribution and optimizes the expectation over costs and constraint violations. Oftentimes, they optimize a feedback policy, rather than a control sequence. Our method, PAC-NMPC, falls into this category of approaches. Early approaches focused on a local iterative solution to the stochastic Hamilton-Jacobi-Bellman equation [21], [22], which relies on a first order approximation of the dynamics for noise propagation. Stochastic differential dynamic programming approaches [23] would later allow for second order approximation of the dynamics. More recent methods utilize the unscented transform to propagate noise through nonlinear dynamics [8], [24]. In [25], the authors leverage path integral control to generate open-loop trajectories and create a sampling-based NMPC algorithm. More recent extensions [26], [9] include a feedback policy for robust performance. [27] provides guarantees on free-energy growth.

Sampling-based stochastic optimal control methods are closely related to policy search in reinforcement learning. A general background and survey of common policy search methods can be found in [28]. In [11], researchers developed an approach for robust policy search using a Probably Approximately Correct (PAC) learning framework called PAC Robust Policy Search (PROPS) based on recently derived sample complexity bounds in [10]. Researchers have also recently explored (PAC)-Bayes theory to generate collision-avoidance policies with performance guarantees in novel environments [29] and achieve vision-based planning with motion primitives [30]. Our PAC-NMPC method builds on the work in [11] and [10] to develop a highly generalizable sampling-based stochastic feedback motion-planning algorithm that can provide statistical performance guarantees for a large class of uncertain dynamical systems.

III. APPROACH

A. Trajectory Optimization

1) *Formulation:* We formulate trajectory optimization as stochastic policy optimization (Alg. 1). Specifically, we optimize the hyperparameters of a distribution over the control trajectory, $\xi_{ij} \sim p(\cdot|\nu_i)$. Control trajectories are sampled from the distribution, evaluated with cost and constraint functions, and used to improve the distribution hyperparameters. This process iterates until a termination condition is reached.

We directly optimize sample complexity bounds [10] over the expected costs and constraints (Eq. 1). We specify a constraint weight, γ , the number of prior policies, L , the number of samples, M , and the bound confidence, $1 - \delta$.

$$\begin{aligned} \text{optimize}(\nu, \xi, \mathbf{J}, \mathbf{I}) &= \arg \min_{\nu} \min_{\alpha > 0} (\mathcal{J}_{\alpha}^{+}(\nu) + \gamma \mathcal{I}_{\alpha}^{+}(\nu)) \\ \mathcal{J}_{\alpha}^{+}(\nu) &\triangleq \widehat{\mathcal{J}}_{\alpha}(\nu) + \mathcal{J}_D(\nu) + \frac{1}{\alpha LM} \log \frac{1}{\delta} \\ \widehat{\mathcal{J}}_{\alpha}(\nu) &\triangleq \frac{1}{\alpha LM} \sum_{i=0}^{L-1} \sum_{j=1}^M \psi(\alpha \ell_i(\xi_{ij}, \nu)) \\ \psi(x) &= \log \left(1 + x + \frac{1}{2} x^2 \right) \\ \ell_i(\xi_{ij}, \nu) &= J_{ij} \frac{p(J_{ij}|\bar{\nu})}{p(J_{ij}|\nu_i)} = J_{ij} \frac{p(\xi_{ij}|\bar{\nu})}{p(\xi_{ij}|\nu_i)} \end{aligned} \quad (1)$$

Algorithm 1: PAC Trajectory Distribution Opt.

```

1 Inputs:  $\nu_0$  ; // Initial prior distribution
2  $i \leftarrow 0, \nu \leftarrow \cdot, \xi \leftarrow \{\}, \mathbf{J} \leftarrow \{\}, \mathbf{I} \leftarrow \{\}$ ;
3 while time allows do
4    $\xi_i \leftarrow \{\}, \mathbf{J}_i \leftarrow \{\}, \mathbf{I}_i \leftarrow \{\}$ ;
5   for  $j = 1, \dots, M$  do // GPU Parallelized
6      $\xi_{ij} \sim p(\cdot|\nu_i)$  ; // Sample trajectory
7      $J_{ij}, I_{ij} \sim p(\cdot|\xi_{ij})$  ; // Eval cost/constraint
8      $\xi_i.append(\xi_{ij}), \mathbf{J}_i.append(J_{ij}), \mathbf{I}_i.append(I_{ij})$ ;
9    $\nu.append(\nu_i), \xi.append(\xi_i), \mathbf{J}.append(\mathbf{J}_i),$ 
10   $\mathbf{I}.append(\mathbf{I}_i)$ ;
11   $\nu_{i+1} = \text{optimize}(\nu, \xi, \mathbf{J}, \mathbf{I})$  ; // Optimize dist.
12   $i \leftarrow i + 1$ ;
13 return  $\nu_i$ 
```

$$\mathcal{J}_D(\nu) \triangleq \frac{\alpha}{2L} \sum_{i=0}^{L-1} \max(\mathbf{J}_i)^2 e^{D_2(p(\cdot|\bar{\nu})||p(\cdot|\nu_i))}$$

$$D_{\beta}(p||q) = \frac{1}{\beta - 1} \log \int \frac{p^{\beta}(x)}{q^{\beta-1}(x)} dx$$

We require an analytical control trajectory distribution to better manage the hyperparameters and facilitate the computation of the Renyi divergence, D_2 . By contrast, the only requirement on the cost and constraint distributions, $J_{ij}, I_{ij} \sim p(\cdot|\xi_{ij})$, is to permit sampling. This property enables the use of very complex (potentially “black-box”) cost and constraint distributions, and allows our algorithm to generalize to a large class stochastic dynamics models and probabilistic constraints.

We parameterize the trajectory distribution as a multivariate Gaussian over a discrete sequence of control actions. Each dimension of the Gaussian describes a control action at a timestep in the trajectory. Thus, the distribution over a control trajectory with an N -dimensional control input and T timesteps is parameterized as a NT -dimensional multivariate Gaussian. The mean and covariance of this distribution are used as hyperparameters (Eq. 2). We assume a diagonal covariance matrix for computational efficiency.

$$\begin{aligned} \nu &= [\mu, \sigma^2] \in \mathcal{R}^{2*N*T}, \mu \in \mathcal{R}^{N*T}, \sigma^2 \in \mathcal{R}^{N*T} \\ p(\xi|\nu) &= p(\xi \sim \mathcal{N}(\mu, \text{diag}(\sigma^2))) \end{aligned} \quad (2)$$

Our cost/constraint sampling functions are broken down into two stages: rollout using stochastic dynamics, $p(\mathbf{x}_k|\mathbf{x}_{k-1}, \mathbf{u}_{k-1})$, into state space, and evaluation (Alg. 2).

Algorithm 2: Cost/Constraint Sampling

```

1 Inputs:  $\mathbf{x}_0, \xi_{ij}$  ; // Init state and control traj
2  $\mathbf{u} = \xi_{ij}, \mathbf{x} \leftarrow \{\mathbf{x}_0\}$ ;
3 for  $k = 1, \dots, T$  do // Stochastic Rollout
4    $\mathbf{x}_k \sim p(\cdot|\mathbf{x}_{k-1}, \mathbf{u}_{k-1})$  ; // Sample next state
5    $\mathbf{x}.append(\mathbf{x}_k)$ ;
6  $J_{ij}, I_{ij} = \text{cost\_constr}(\mathbf{u}, \mathbf{x})$  ; // Eval cost/constr.
7 Return  $J_{ij}, I_{ij}$ 
```

2) *Experiment:* We simulate a stochastic bicycle model with acceleration and steering rate inputs:

$$\begin{aligned} \dot{x}_0 &= x_3 \cos(x_2) + \omega_0 & \dot{x}_3 &= u_0 + \omega_3 \\ \dot{x}_1 &= x_3 \sin(x_2) + \omega_1 & \dot{x}_4 &= u_1 + \omega_4 \\ \dot{x}_2 &= x_3 \tan(x_4)/L + \omega_2 \end{aligned} \quad (3)$$

where $\mathbf{x} = [x_0, x_1, x_2, x_3, x_4]$ is the state vector, $\mathbf{u} = [u_0, u_1]$ is the control vector, $L = 0.33$ is the wheel base, and $\omega \sim \mathcal{N}(0, \Sigma)$, $\Sigma = \text{diag}([0.001, 0.001, 0.1, 0.2, 0.001])$. Euler integration is used to discretize the dynamics.

A 20 timestep trajectory with $\Delta t = 0.1$ sec is optimized, with an initial state of $\mathbf{x}_I = [0.0, 0.0, 0.0, 1.0, 0.0]$ and a goal state of $\mathbf{x}_G = [3.0, 0.0, 0.0, 1.0, 0.0]$. The steering angle is constrained to $(-0.4, 0.4)$ rad, the steering rate to $(-1.0, 1.0) \frac{\text{rad}}{\text{sec}}$, and the acceleration to $(-1.0, 1.0) \frac{\text{m}}{\text{s}^2}$. We apply a quadratic cost of the form $J = \mathbf{x}_T^T \mathbf{Q}_f \mathbf{x}_T$ where $\mathbf{Q}_f = \text{diag}([2.0, 2.0, 0.0, 0.0, 0.0])$. An obstacle constraint is applied with circular obstacles at $(1.0, 0.75)$ and $(2.0, -0.75)$. Our prior distribution has a mean of all zeros and a variance of all ones. Parameters were as follows: $L = 5$, $M = 1024$, $\delta = 0.05$, $\gamma = 10$. We used a GPU implementation of L-BFGS-B for distributed optimization [31]. Simulations were run on a laptop with an Intel Core i9-9880H CPU and a Nvidia GeForce RTX 2070 GPU.

The trajectory distribution converged to an expected cost bound of 1.01 and a probability of collision bound of 8.23% (Fig. 2). Each iteration took approximately 15.9 ms. At each iteration, these bounds were compared to estimates of the expected cost and probability of collision. The estimates were constructed through Monte Carlo sampling of 1024 trajectories (Fig 3).

We also optimized the PAC bounds with deterministic dynamics and compared to Monte Carlo estimates sampled with stochastic dynamics. This caused the probability of collision estimates to no longer be properly bounded (Fig. 2), thus highlighting the necessity of properly considering stochasticity to generate accurate statistical guarantees.

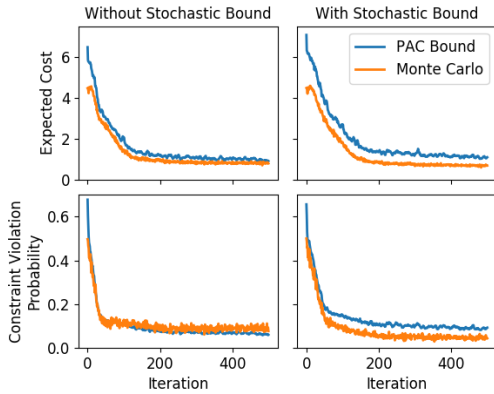


Fig. 2. Convergence of PAC Bound compared to Monte Carlo estimates. Left plots optimize bounds with deterministic dynamics, right plots optimize bounds using stochastic dynamics. Monte Carlo estimates are evaluated with stochastic dynamics.

B. Feedback

1) *Formulation*: To incorporate a feedback policy, we employ a two-stage sampling process and evaluate the response of local tracking controllers to disturbances. In the first stage, we rollout control trajectory samples with the nominal dynamics, \bar{f} , and compute feedback parameters, \mathbf{K} , using the resulting nominal state trajectory. In the second stage,

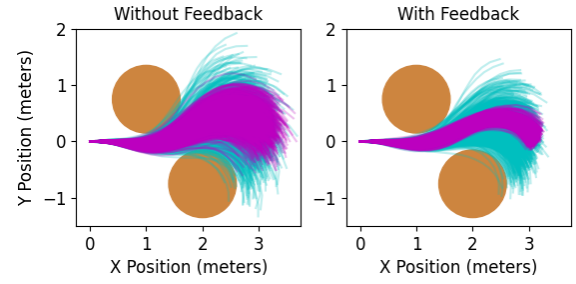


Fig. 3. Samples from optimized control trajectory distribution and stochastic dynamics in cyan. Samples from mean of distribution and stochastic dynamics in magenta. Obstacles in brown.

we rollout the closed-loop stochastic dynamics regulated by controller, $\mathbf{u}_k = \psi(\mathbf{x}_k, \bar{\mathbf{x}}_k, \bar{\mathbf{u}}_k, \mathbf{K})$ (Alg. 3).

Algorithm 3: Cost/Constraint Sampling with Feedback

```

1 Inputs:  $\mathbf{x}_0, \xi_{ij}$ ; // Init state and control traj
2  $\bar{\mathbf{u}} = \xi_{ij}$ ,  $\bar{\mathbf{x}} \leftarrow \{\mathbf{x}_0\}$ ;
3 for  $k = 1, \dots, T$  do // Deterministic Rollout
4    $\bar{\mathbf{x}}_k = \bar{f}(\bar{\mathbf{x}}_{k-1}, \bar{\mathbf{u}}_{k-1})$ ;
5    $\bar{\mathbf{x}}.append(\bar{\mathbf{x}}_k)$ ;
6  $\mathbf{K} = \text{ComputeFeedbackParams}(\bar{\mathbf{x}}, \bar{\mathbf{u}})$ ;
7  $\mathbf{x} \leftarrow \{\mathbf{x}_0\}$ ;
8 for  $k = 1, \dots, T$  do // Stochastic Rollout
9    $\mathbf{u}_{k-1} = \psi(\mathbf{x}_{k-1}, \bar{\mathbf{x}}_{k-1}, \bar{\mathbf{u}}_{k-1}, \mathbf{K})$ ;
10   $\mathbf{x}_k \sim p(\cdot | \mathbf{x}_{k-1}, \mathbf{u}_{k-1}, \Sigma)$ ;
11   $\mathbf{x}.append(\mathbf{x}_k)$ ;
12  $J_{ij}, I_{ij} = \text{cost\_constr}(\mathbf{u}, \mathbf{x})$ ; // Eval cost/constraint
13 Return  $J_{ij}, I_{ij}$ 
```

We use the finite horizon, discrete, time varying linear quadratic regulator (TVLQR) as a feedback controller [32]:

$$\mathbf{u}_k = \psi(\mathbf{x}_k, \bar{\mathbf{x}}_k, \bar{\mathbf{u}}_k, \mathbf{K}) = \mathbf{K}(\mathbf{x}_k - \bar{\mathbf{x}}_k) + \bar{\mathbf{u}}_k \quad (4)$$

For each sampled nominal trajectory, the feedback parameters, \mathbf{K} , are computed by integrating the finite horizon discrete Riccati equations backwards in time using locally linearized dynamics.

2) *Experiment*: We used the following feedback costs: $\mathbf{Q}' = \text{diag}[10.0, 10.0, 1.0, 1.0, 1.0]$, $\mathbf{R}' = \text{diag}([1.0, 1.0])$, $\mathbf{Q}'_f = \text{diag}([100.0, 100.0, 10.0, 10.0, 10.0])$. Otherwise, all parameters are the same as previously stated.

While using feedback, the trajectory distribution converged to an expected cost bound of 0.743 and a probability of collision bound of 5.36% (Fig. 4). Each iteration took approximately 18.5 ms. As shown in the Monte Carlo trajectory samples (Fig. 3) and reduced bound values, the feedback policy improved performance.

In this experiment, we do not observe many bound violations when optimizing the PAC bounds with deterministic dynamics because the feedback policy is compensating for the stochastic dynamics during Monte Carlo sampling. However, the estimated expected cost and probability of collision were still able to converge to smaller values when optimizing with stochastic dynamics: 0.500 vs 0.636 and 0.78% vs 2.54%, respectively.

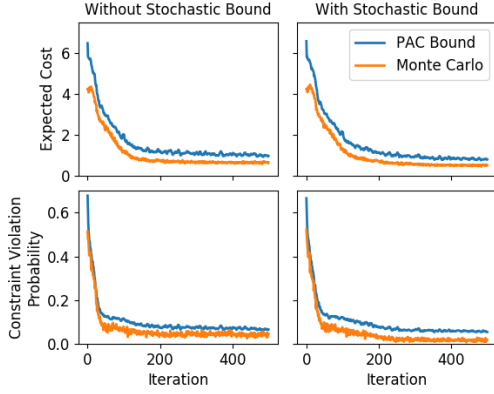


Fig. 4. Convergence of PAC Bound compared to Monte Carlo estimates while using feedback.

C. NMPC

1) *Formulation:* The proposed trajectory distribution optimization is used as a basis for PAC-NMPC (Alg. 4). At each planning interval, with a period of H , the control trajectory distribution is optimized given the current state estimate, \mathbf{x}_0 , and prior hyperparameters, ν_0 . From the optimized distribution, ν^* , a control trajectory is sampled, rolled out into state space, and used to compute feedback parameters. The trajectory and feedback parameters are the trimmed by $\frac{H}{\Delta t}$ to account for time passed since the beginning of the planning interval. The resulting feedback policy is then yielded for execution.

Algorithm 4: PAC-NMPC

```

1 Input:  $\nu^* \leftarrow \nu_0$ ; // Initial Distribution
2 while goal not reached do
3    $\mathbf{x}_0 = \text{GetCurrentStateEstimate}()$ ;
4    $\nu_0 = \text{CreatePrior}(\nu^*, \mathbf{x}_0)$ ;
5    $\nu^* = \text{TrajectoryDistributionOpt}(\nu_0, \mathbf{x}_0)$ ;
6    $\bar{\mathbf{u}} = \text{Sample}(\nu^*)$ ;
7    $\bar{\mathbf{x}} \leftarrow \{\mathbf{x}_0\}$ ;
8   for  $k = 1, \dots, T$  do // Deterministic Rollout
9      $\bar{\mathbf{x}}_k = \bar{f}(\bar{\mathbf{x}}_{k-1}, \bar{\mathbf{u}}_{k-1})$ ;
10     $\bar{\mathbf{x}}.append(\bar{\mathbf{x}}_k)$ ;
11    $\mathbf{K} = \text{ComputeFeedbackParams}(\bar{\mathbf{x}}, \bar{\mathbf{u}})$ ;
12    $\bar{\mathbf{u}}, \bar{\mathbf{x}}, \mathbf{K} \leftarrow \text{Trim}(\bar{\mathbf{u}}, \bar{\mathbf{x}}, \mathbf{K})$ ;
13   Yield  $(\bar{\mathbf{u}}, \bar{\mathbf{x}}, \mathbf{K})$ ;
14 Return
```

Given that optimal trajectory distributions are expected to be similar between subsequent planning intervals, we use the optimal hyperparameters from the last planning iteration to initialize the new prior hyperparameters. This initialization is extremely important since it allows the prior to start near an optimal solution, thus reducing the required number of iterations for convergence.

For PAC-NMPC to be effective, the hyperparameters describing the first $\frac{H}{\Delta t}$ timesteps of the trajectory distribution should represent control signals that the system is currently executing and should not be modified during the optimization process. Since we initialize our prior with hyperparameters from the last planning interval, i.e. the commands currently

being executed, we simply do not optimize the hyperparameters associated with these timesteps.

In our experiment, we execute the mean trajectory from the optimized distributions. This is not only the most likely sample, but is also trivial to compute given our multivariate Gaussian representation:

$$\bar{\mathbf{u}} = \text{Sample}(\nu^*) = \mu^*$$

Trimming the sampled trajectory and feedback parameters is simple:

$$\bar{\mathbf{u}}, \bar{\mathbf{x}}, \mathbf{K} \leftarrow \text{Trim}(\bar{\mathbf{u}}, \bar{\mathbf{x}}, \mathbf{K}) = \bar{\mathbf{u}}_{\frac{H}{\Delta t}:T}, \bar{\mathbf{x}}_{\frac{H}{\Delta t}:T}, \mathbf{K}_{\frac{H}{\Delta t}:T}$$

The multivariate Gaussian hyperparameter representation also simplifies initialization of the prior for the next planning iteration. To do so, we trim the hyperparameters, run the mean trajectory through the feedback controller, pad the mean trajectory with zeros, and extend the variance trajectory (see Algo. 5).

Algorithm 5: Create Prior

```

1 Input:  $\nu^*, \mathbf{x}_0$ ; // Hyperparameters, Initial State
2  $[\bar{\mu}, \bar{\sigma}^2] = \nu^*$ ; // Mean and Variance Trajectories
3  $\bar{\mu}, \bar{\sigma}^2 \leftarrow \text{Trim}(\bar{\mu}, \bar{\sigma}^2)$ ,  $\bar{\mathbf{x}} \leftarrow \{\mathbf{x}_0\}$ ;
4 for  $k = 1, \dots, T - \frac{H}{\Delta t}$  do // Determ. Rollout
5    $\bar{\mathbf{x}}_k = \bar{f}(\bar{\mathbf{x}}_{k-1}, \bar{\mu}_{k-1})$ ;
6    $\bar{\mathbf{x}}.append(\bar{\mathbf{x}}_k)$ ;
7  $\mathbf{K} = \text{ComputeFeedbackParams}(\bar{\mathbf{x}}, \bar{\mu})$ ;
8  $\mathbf{x} \leftarrow \{\bar{\mathbf{x}}_0\}$ ;
9  $\mu \leftarrow \{\}$ ;
10 for  $k = 1, \dots, T - \frac{H}{\Delta t}$  do // Stochastic Rollout
11    $\mu_{k-1} = \psi(\mathbf{x}_{k-1}, \bar{\mathbf{x}}_{k-1}, \bar{\mu}_{k-1}, \mathbf{K})$ ;
12    $\mathbf{x}_k \sim p(\cdot | \mathbf{x}_{k-1}, \mu_{k-1}, \Sigma)$ ;
13    $\mu.append(\mu_{k-1})$ ;
14    $\mathbf{x}.append(\mathbf{x}_k)$ ;
15 for  $k = 1, \dots, \frac{H}{\Delta t}$  do // Pad Mean, Extend Var.
16    $\mu.append(\mathbf{0})$ ;
17    $\sigma^2.append(\sigma_{T-\frac{H}{\Delta t}}^2)$ ;
18 Return  $[\mu, \sigma^2]$ 
```

2) *Experiment:* The system follows a receding horizon point generated on a looping path. The path runs along a set of circular obstacles. We optimize a 12 timestep trajectory with $\Delta t = 0.1$ sec at a replanning period of $H = 0.2$ sec. We apply a quadratic cost of the form $J = \mathbf{x}_T^T \mathbf{Q}_f \mathbf{x}_T$ where $\mathbf{Q}_f = \text{diag}([1.0, 1.0, 0.1, 0.1, 0.0])$. Parameters were as follows: $L = 5$, $M = 1024$, $\delta = 0.05$, $\gamma = 10$. One small relaxation that we make is to interpolate the sampled control trajectory from 10Hz to 50Hz and assume that our PAC bounds will still hold. This allows us to control the system at higher rate.

We perform an ablation study in which we compare performance with and without feedback, as well as optimizing the PAC bounds with and without stochastic dynamics.

PAC-NMPC was successfully able to control the system in real time and followed the path while avoiding nearby obstacles. In Figure 5, we show the route taken by the system during five loops of the path. It also shows a quantitative difference in the path when we ablate stochastic dynamics in the bound optimization, feedback, or both.

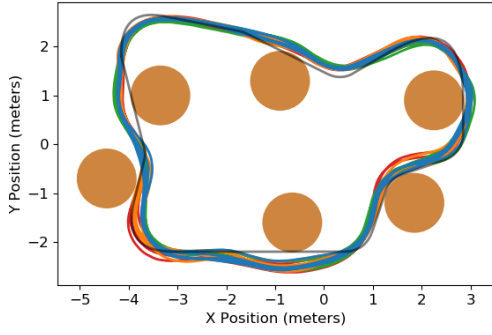


Fig. 5. Paths taken while following route (black) and avoiding obstacles (brown) in simulation. Blue/green paths use stochastic bounds, red/orange paths do not. Blue/orange paths use feedback, red/green paths do not.

During each planning interval of $H = 0.2$ sec, the controller achieved an average of 54 iterations of trajectory distribution optimization (approximately 3.7ms per iteration). The controller consistently produced PAC bounds of around 5% probability of collision, which accurately bounded the Monte Carlo estimates. The bound was exceeded only once out of 482 planning intervals. Thus, the estimates were bounded accurately in around 99.8% of planning intervals, well within the 95% confidence bound (Fig 6).

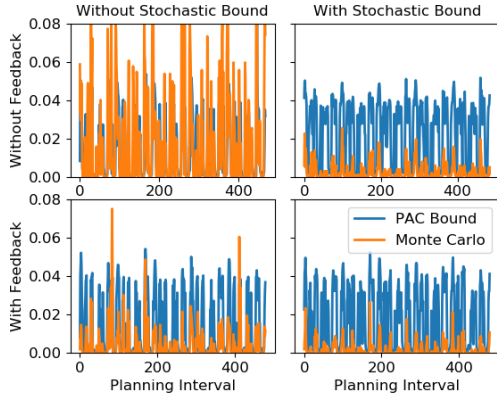


Fig. 6. Optimized PAC Bound compared to Monte Carlo estimates for probability of constraint violation at each planning interval.

When optimizing the bounds with deterministic dynamics, the probability of collision estimates were only bounded in 93.9% of planning intervals. This decrease in bound accuracy is even more apparent when running the controller without feedback to compensate for unmodeled noise; optimizing with deterministic dynamics without feedback results in only 64.7% of planning intervals having bounded probability of collision estimates (Fig 6).

IV. HARDWARE EXPERIMENTS

A. Hardware

To evaluate our method on physical hardware, we ran PAC-NMPC on a 1/10th-scale Traxxas Rally Car platform (Fig. 7(a)). The algorithm runs on a Nvidia Jetson Orin mounted on the bottom platform. The control interface is a variable electronic speed controller (VESC), which executes commands and provides servo state information. The position and orientation is tracked with an OptiTrack system.

B. Setup

The route, virtual obstacle placements, and TVLQR costs are identical to those in the simulation experiments. We optimize a 12 timestep trajectory with $\Delta t = 0.1$ sec at a replanning period of $H = 0.2$ sec. We apply a quadratic cost to the final state of the form $J = \mathbf{x}_T^T \mathbf{Q}_f \mathbf{x}_T$ where $\mathbf{Q}_f = \text{diag}([1.0, 1.0, 0.4, 0.1, 0.0])$. Parameters were as follows: $L = 2$, $M = 1024$, $\delta = 0.05$, $\gamma = 10$.

We model the rally car dynamics as a stochastic bicycle model where noise is modeled as a 3 component Gaussian Mixture Model. This mixture model was fit from data collected with the car (Fig. 7(b)).

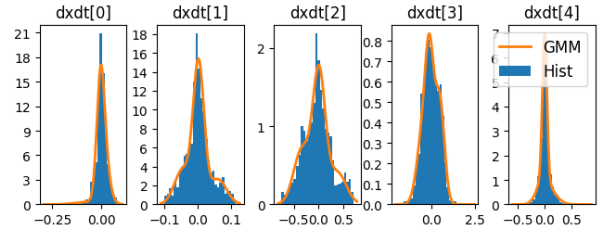


Fig. 7. Rally car platform and dynamics noise model

We perform the same ablation study as done in the simulation experiments.

C. Results

PAC-NMPC was successfully able to run onboard the rally car in real time and followed the path while avoiding nearby obstacles. In Figure 8, we display the path taken by the car.

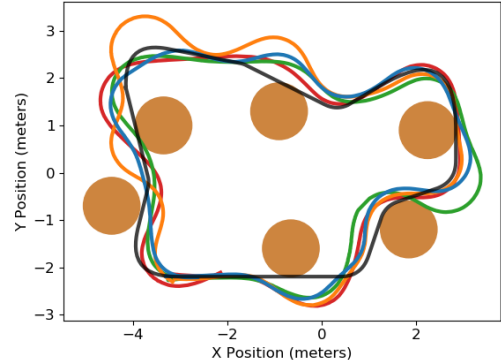


Fig. 8. Path taken while following route (black) and avoiding obstacles (brown) with rally car hardware. Blue/green paths use stochastic bounds, red/orange paths do not. Blue/orange paths use feedback, red/green paths do not.

During each planning interval of $H = 0.2$ sec, the controller achieved an average of 10 iterations of trajectory

distribution optimization (approximately 20ms per iteration). The controller consistently produced PAC bounds of around 10% probability of collision, which accurately bounded the Monte Carlo estimates of the probability of collision at all planning intervals (Fig. 9).

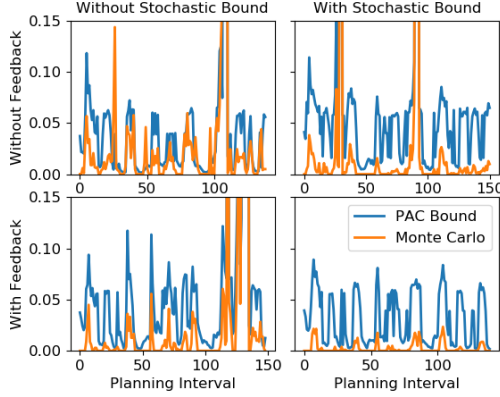


Fig. 9. Optimized PAC Bound compared to Monte Carlo estimates for probability of constraint violation at each planning interval. When the bound/estimate peaks outside of the y-axis view, a collision has likely occurred.

When optimizing the bounds with deterministic dynamics, the probability of collision estimates were bounded in 97.9% of planning intervals. This decrease in bound accuracy is even more apparent when running the controller without feedback to compensate for unmodeled noise; optimizing with deterministic dynamics without feedback results in only 85.1% of planning intervals having bounded probability of collision estimates (Fig. 9).

V. APPLICATION TO FIXED-WING UAVS

A. Setup

To demonstrate that our approach can extend to more complex, high-dimensional systems, we use PAC-NMPC to control a simulated fixed-wing dynamical system. We simulate a quaternion formulation of the fixed-wing described in [2]. This system has a 17-dimensional state space and a 4-dimensional control space. We place zero-mean Gaussian noise over the dynamics with a covariance of

$$\Sigma = \text{diag}([.001, .001, .001, .001, .001, .001, .001, .001, .001, .001, .001, .001, .001, .001, .001, .001, .001])$$

We optimize a 12 timestep trajectory with $\Delta t = 0.1$ sec at a replanning period of $H = 0.2$. We apply a quadratic cost of the form $J = \mathbf{x}_T^T \mathbf{Q}_f \mathbf{x}_T + \sum_{i=1}^{T-1} \mathbf{x}_i^T \mathbf{Q} \mathbf{x}_i$ and an obstacle constraint. Parameters were as follows: $L = 1$, $M = 1024$, $\delta = 0.05$, and $\gamma = 10$. We use feedback and use stochastic dynamics to optimize the PAC bounds. The state costs were:

$$\mathbf{Q} = \text{diag}([0, 0, 0, 0, 0, 0, 0, 0, 1, 1, 1, 0, 0, 0, 0, 0, 0])$$

$$\mathbf{Q}_f = \text{diag}([.1, .1, .1, .1, .5, .5, .5, .1, .1, .1, .01, .01, .01, .01, .01, .01, .01])$$

The TVLQR costs were:

$$\mathbf{Q}' = \text{diag}([25, 25, 25, 50, 50, 50, 50, 2, 2, 2, 2, 2, 2, 2, 2, 2, 2])$$

$$\mathbf{Q}'_f = \text{diag}([100, 100, 100, 100, 100, 100, 100, 1, 1, 1, 1, 1, 1, 1, 1, 1, 1])$$

$$\mathbf{R}' = \text{diag}(1, 1, 1, 25)$$

To enable real time performance, we compute the linearized dynamics for the feedback policy using finite difference on the mean trajectory of the latest prior distribution.

This still results in valid PAC bounds since the number of prior policies, L , is set to one. This simulation was run on a desktop computer with an AMD Ryzen 7 5800x and a NVIDIA GeForce RTX 3080.

B. Results

PAC-NMPC was successfully able to control the simulated fixed-wing in real time, following the path while avoiding nearby obstacles. In Figure 10, we display the route taken by the system during five loops of the path.

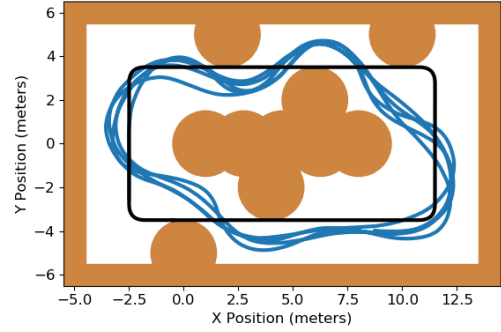


Fig. 10. Path taken while following route (black) and avoiding obstacles (brown) with fixed-wing simulation.

During each planning interval of $H = 0.2$ sec, the controller achieved an average of 24 iterations of trajectory distribution optimization (approximately 8.3ms per iteration). The controller consistently produced PAC bounds of less than 15% probability of collision, which accurately bounded the Monte Carlo estimates (Fig. 11).

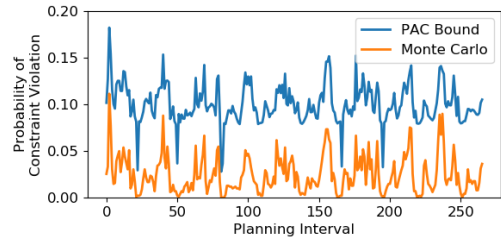


Fig. 11. Optimized PAC Bound compared to Monte Carlo estimates for probability of constraint violation.

VI. DISCUSSION

In this work, we presented a novel SNMPC method capable of propagating uncertainty through arbitrary nonlinear dynamic systems and of providing statistical guarantees on expected cost and constraint violations. We demonstrated real time performance both in simulation and on-board physical hardware. Further, we show that the algorithm is capable of scaling to more complex systems, like fixed-wing UAVs. Since this algorithm can be used with “black-box” sampling of dynamics (assuming they are continuously differentiable), costs, constraints, and noise, future work can investigate its use with learned dynamics and perception-informed costs. Future work could also explore the extension of this approach to more complex control trajectory distributions.

REFERENCES

- [1] D. Falanga, P. Foehn, P. Lu, and D. Scaramuzza, "Pampc: Perception-aware model predictive control for quadrotors," in *2018 IEEE/RSJ International Conference on Intelligent Robots and Systems (IROS)*. IEEE, 2018, pp. 1–8.
- [2] M. Basescu and J. Moore, "Direct nmpp for post-stall motion planning with fixed-wing uavs," in *2020 IEEE International Conference on Robotics and Automation (ICRA)*. IEEE, 2020, pp. 9592–9598.
- [3] Y. Ding, A. Pandala, and H.-W. Park, "Real-time model predictive control for versatile dynamic motions in quadrupedal robots," in *2019 International Conference on Robotics and Automation (ICRA)*. IEEE, 2019, pp. 8484–8490.
- [4] R. Grandia, F. Farshidian, R. Ranftl, and M. Hutter, "Feedback mpc for torque-controlled legged robots," in *2019 IEEE/RSJ International Conference on Intelligent Robots and Systems (IROS)*. IEEE, 2019, pp. 4730–4737.
- [5] J. A. Paulson and A. Mesbah, "An efficient method for stochastic optimal control with joint chance constraints for nonlinear systems," *International Journal of Robust and Nonlinear Control*, vol. 29, no. 15, pp. 5017–5037, 2019.
- [6] Z. Manchester and S. Kuindersma, "Dirtrel: Robust trajectory optimization with ellipsoidal disturbances and lqr feedback," in *Robotics: Science and Systems*. Cambridge, MA, USA, 2017.
- [7] S. Singh, A. Majumdar, J.-J. Slotine, and M. Pavone, "Robust online motion planning via contraction theory and convex optimization," in *2017 IEEE International Conference on Robotics and Automation (ICRA)*. IEEE, 2017, pp. 5883–5890.
- [8] N. Ozaki, S. Campagnola, and R. Funase, "Tube stochastic optimal control for nonlinear constrained trajectory optimization problems," *Journal of Guidance, Control, and Dynamics*, 2020.
- [9] J. Yin, Z. Zhang, E. Theodorou, and P. Tsiotras, "Trajectory distribution control for model predictive path integral control using covariance steering," in *2022 International Conference on Robotics and Automation (ICRA)*. IEEE, 2022, pp. 1478–1484.
- [10] M. Kobilarov, "Sample complexity bounds for iterative stochastic policy optimization," *Advances in Neural Information Processing Systems*, vol. 28, 2015.
- [11] M. Shekells, "Probably approximately correct robust policy search with applications to mobile robotics," Ph.D. dissertation, Johns Hopkins University, 2020.
- [12] M. E. Villanueva, R. Quirynen, M. Diehl, B. Chachuat, and B. Houska, "Robust mpc via min–max differential inequalities," *Automatica*, vol. 77, pp. 311–321, 2017.
- [13] G. Garimella, M. Shekells, J. L. Moore, and M. Kobilarov, "Robust obstacle avoidance using tube nmpp," in *Robotics: Science and Systems*, 2018.
- [14] S. Lucia, R. Paulen, and S. Engell, "Multi-stage nonlinear model predictive control with verified robust constraint satisfaction," in *53rd IEEE Conference on Decision and Control*. IEEE, 2014, pp. 2816–2821.
- [15] D. Q. Mayne, E. C. Kerrigan, E. Van Wyk, and P. Falugi, "Tube-based robust nonlinear model predictive control," *International journal of robust and nonlinear control*, vol. 21, no. 11, pp. 1341–1353, 2011.
- [16] D. L. Marruedo, T. Alamo, and E. F. Camacho, "Input-to-state stable mpc for constrained discrete-time nonlinear systems with bounded additive uncertainties," in *Proceedings of the 41st IEEE Conference on Decision and Control*, 2002., vol. 4. IEEE, 2002, pp. 4619–4624.
- [17] Y. Gao, A. Gray, H. E. Tseng, and F. Borrelli, "A tube-based robust nonlinear predictive control approach to semiautonomous ground vehicles," *Vehicle System Dynamics*, vol. 52, no. 6, pp. 802–823, 2014.
- [18] F. Bayer, M. Bürger, and F. Allgöwer, "Discrete-time incremental iss: A framework for robust nmpp," in *2013 European Control Conference (ECC)*. IEEE, 2013, pp. 2068–2073.
- [19] G. Chou, N. Ozay, and D. Berenson, "Model error propagation via learned contraction metrics for safe feedback motion planning of unknown systems," in *2021 60th IEEE Conference on Decision and Control (CDC)*. IEEE, 2021, pp. 3576–3583.
- [20] J. Köhler, R. Soloperto, M. A. Müller, and F. Allgöwer, "A computationally efficient robust model predictive control framework for uncertain nonlinear systems," *IEEE Transactions on Automatic Control*, vol. 66, no. 2, pp. 794–801, 2020.
- [21] E. Todorov and W. Li, "A generalized iterative lqg method for locally-optimal feedback control of constrained nonlinear stochastic systems," in *Proceedings of the 2005, American Control Conference*, 2005. IEEE, 2005, pp. 300–306.
- [22] E. Todorov and Y. Tassa, "Iterative local dynamic programming," in *2009 IEEE Symposium on Adaptive Dynamic Programming and Reinforcement Learning*. IEEE, 2009, pp. 90–95.
- [23] E. Theodorou, Y. Tassa, and E. Todorov, "Stochastic differential dynamic programming," in *Proceedings of the 2010 American Control Conference*. IEEE, 2010, pp. 1125–1132.
- [24] T. A. Howell, C. Fu, and Z. Manchester, "Direct policy optimization using deterministic sampling and collocation," *IEEE Robotics and Automation Letters*, vol. 6, no. 3, pp. 5324–5331, 2021.
- [25] G. Williams, P. Drews, B. Goldfain, J. M. Rehg, and E. A. Theodorou, "Aggressive driving with model predictive path integral control," in *2016 IEEE International Conference on Robotics and Automation (ICRA)*. IEEE, 2016, pp. 1433–1440.
- [26] G. Williams, B. Goldfain, P. Drews, K. Saigol, J. M. Rehg, and E. A. Theodorou, "Robust sampling based model predictive control with sparse objective information," in *Robotics: Science and Systems*, 2018.
- [27] M. S. Gandhi, B. Vlahov, J. Gibson, G. Williams, and E. A. Theodorou, "Robust model predictive path integral control: Analysis and performance guarantees," *IEEE Robotics and Automation Letters*, vol. 6, no. 2, pp. 1423–1430, 2021.
- [28] M. P. Deisenroth, G. Neumann, J. Peters *et al.*, "A survey on policy search for robotics," *Foundations and Trends® in Robotics*, vol. 2, no. 1–2, pp. 1–142, 2013.
- [29] A. Majumdar, A. Farid, and A. Sonar, "Pac-bayes control: learning policies that provably generalize to novel environments," *The International Journal of Robotics Research*, vol. 40, no. 2–3, pp. 574–593, 2021.
- [30] S. Veer and A. Majumdar, "Probably approximately correct vision-based planning using motion primitives," in *Conference on Robot Learning*. PMLR, 2021, pp. 1001–1014.
- [31] Y. Fei, G. Rong, B. Wang, and W. Wang, "Parallel l-bfgs-b algorithm on gpu," *Computers & graphics*, vol. 40, pp. 1–9, 2014.
- [32] R. Tedrake, *Underactuated Robotics*, 2022. [Online]. Available: <http://underactuated.mit.edu>